USING AN INERTIAL SATELLITE NAVIGATION SYSTEM FOR DETERMINATION OF MOTION PARAMETERS OF THE RADAR ANTENNA PHASE CENTER

A.V. Chernodarov[1], A.P. Patrikeev[2]
NaukaSoft Experimental Laboratory, Ltd., 6A, 8 March 4th St., 125167, Moscow, Russia,
Tel: +7 495 2553635, Fax: +7 499 5580049, e-mail: chernod@mail.ru

V.N. Kovregin[3], G.M. Kovregina[4]
"Zaslon" JSC, 9, Kolya Tomchak St., 196084, St. Petersburg, Russia,
Tel: +7 812 3279099, e-mail: g_kovregina@mail.ru

Abstract

Keywords: radar system, aperture synthesis, path instabilities, micronavigation

A technology for estimation of and compensation for path instabilities of a synthetic-aperture radar (SAR) with the use of a distributed micronavigation system (DMNS) is considered. The implementation of such a technology relies on the mutual support of inertial, satellite, and radar systems. For increasing the accuracy of estimation of DMNS errors, the use of combined procedures of filtering and smoothing of observations also on the interval of aperture synthesis is proposed. The results of flight development of the DMNS are presented, which corroborate the fact that it is possible and expedient to apply the proposed technology for increasing the SAR resolution.

Analysis of a Radar Inertial Satellite Navigation System as the Object of Flight Development

At present, the problem [1] of increasing the resolution of radar systems (RADSs) when large areas of the Earth surface are scanned from board an aircraft still remains topical. It is well known [1] that the angular resolution $\delta\Theta$ and the linear resolution δl at the distance D to an object are determined by the relations $\delta\Theta = \lambda / d$ and $\delta l = D\delta\Theta = \lambda D / d$, where λ is the wavelength of the RADS electromagnetic radiation; d is the antenna size.

The solution of the above-mentioned problem through a hardware-based increase of the antenna size is apparently not always feasible due to restrictions on the mass and overall dimensions of aircraft equipment. Because of this, an analytic completion of the directional pattern is implemented by "sewing together" the images that are obtained by an airborne RADS in the path of aircraft motion. With such a RADS aperture synthesis, the need arises for compensation for the distortions of a combined image due to path instabilities caused by aircraft deviation from the rectilinear motion. A schematic representation of motion of the RADS antenna phase center (APC) is shown in Fig. 1, where $oxyz$ is the aircraft body-fixed coordinate frame; $o\xi\eta$ is the reference moving frame [2]; AB is the antenna beam; D is the distance from the APC to the ground surface. The position of a RADS scanned area is determined by the azimuth α and the angle β of the directional-pattern elevation, and the distance is determined by the delay $\tau = 2D / c$ of a signal, where C is the radio propagation velocity. In the present paper, a side-looking RADS is dealt with, in which the angles α and β are constant ones on the synthesis interval. When the aircraft deviates from the reference path, the need arises for determining the increments ΔD in distance with reference to its base value D_0.

The path instabilities on the scan interval can be determined with the use of a strapdown inertial satellite micronavigation system that is placed near the antenna phase center. To compensate for the above instabilities, their estimates are converted into corrections to RADS signals.

Requirements for accuracy characteristics of the micronavigation system for a SAR result from the fact that the errors of determining both the distance D and the difference $\Delta\varphi$ in phases of the emitted and received signals are interrelated. The phase difference depends on the delay τ of a signal, which is connected with the measured distance by the following relation:

$$\Delta\varphi = \omega_0\tau = 2\pi f_0\tau = 2\pi\frac{c}{\lambda}\tau .$$

From relation (1) it is obvious that for the centimeter-wave band and millimeter distance variations due to path instabilities, phase difference changes may reach tens of degrees. Thus, for the centimeter-wave band,

[1] Dr.Tech. Sc., Ass. Prof., Leading Researcher.
[2] Cand. Tech. Sc., Deputy General Director.
[3] Cand. Tech. Sc., Senior Researcher.
[4] Cand. Tech. Sc., Head of Laboratory.

position errors of determining path instabilities on the interval of aperture synthesis are to be at the level of millimeters or several units of centimeters.

The potentialities of a synthetic-aperture radar (SAR) are attained when a micronavigation system is combined with the APC. However, due to design constraints, such conditions for SAR construction are difficult to realize. Therefore, in actual practice, the need arises for integration of data on APC motion, which come from systems that are spaced apart with respect to the APC.

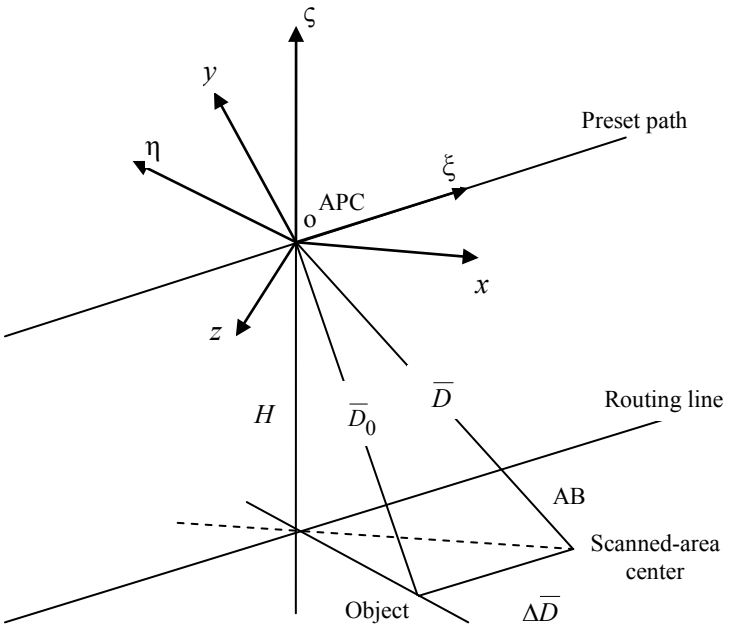

Fig.1. Schematic representation of motion of the RADS antenna phase center

$$D = \frac{c\tau}{2} = \frac{\lambda}{4\pi}\Delta\varphi\,. \tag{1}$$

In [3], consideration has been given to theoretical questions and the results of seminatural studies of the procedures of compensation for path instabilities in SAR signals by the use of a spatially distributed micronavigation system (DMNS). A DMNS breadboard model of technological design, which is shown in Fig. 2 includes the following modules: the IMU-500 sensory package (SP) based on the triad of fiber-optic gyros (FOGs) and accelerometers, which were designed by the ”OPTOLINK“ RPC (Zelenograd); the K-161 receiver of a satellite navigation system (SNS), which was developed by the RIRV (St. Petersburg); a computing module made to the PC-104 standard; power modules; input-output interface modules. In the DMNS, the IMU-500 package is placed near the APC, and path instabilities are calculated in a specialized airborne computer. Figure 3 shows a schematic representation of the DMNS math-based software (MBS) of modular design, where as an addition to the aforesaid, the following notation is introduced: FNPs are flight and navigational parameters; DSINS is a distributed strapdown inertial navigation system; FCNC is a flight-control navigation complex; KBF is a Kalman-Brown filter [4].

For the DMNS to be implemented, the following problems have been solved in [3]:

- kinematic equations that reflect the dynamic behavior of path instabilities on the interval of aperture synthesis were formed from the data of spatially distributed navigational sensors;
- kinematic equations that reflect the dynamic behavior of corrections to RADS signals, which are connected with path instabilities on the interval of aperture synthesis were formed;

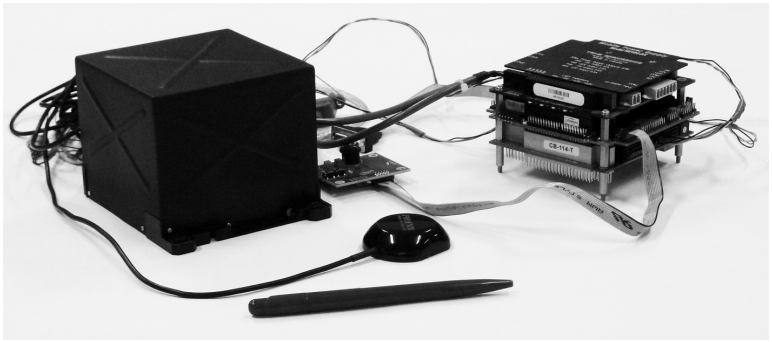

Fig. 2. Breadboard model of the distributed micronavigation system for a SAR

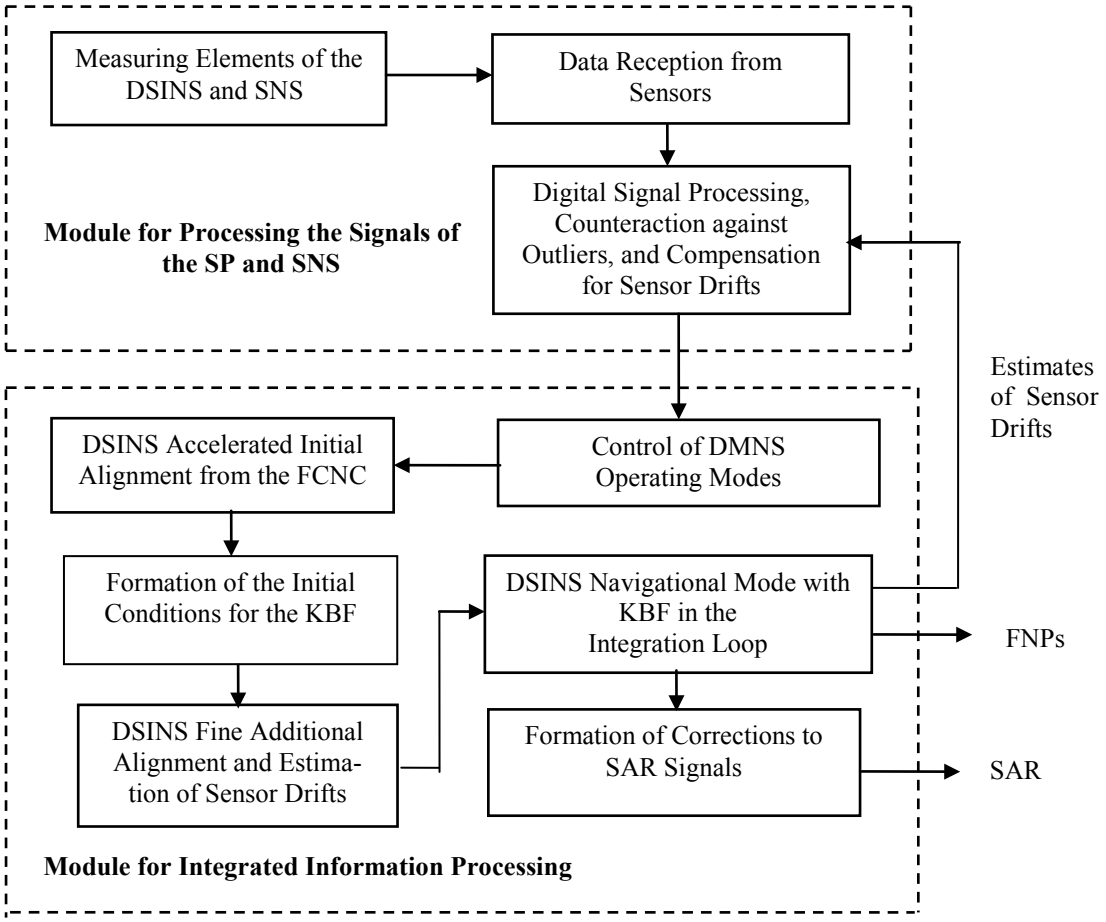

Fig. 3. Block diagram of the DMNS math-based software

- DMNS error equations brought to the level of sensors were formed;
- observations and their models were formed for the application of the Kalman filtering mathematical apparatus in the loop for estimation of DMNS errors.

In [4], for the purpose of increasing the accuracy of APC positioning, the following DMNS actual flight operating conditions have been taken into account:

- the DMNS begins operation only in flight and at the same time as the SAR is switched on. For series-produced strapdown inertial navigation systems (SINS), such an operating mode is the standby or emergency mode and it provides for the alignment and/or additional alignment of a SINS in flight;
- for the application of the Kalman filtering mathematical apparatus, procedures for synchronization of inertial and satellite measurements when estimating DMNS errors have been elaborated, i.e.,

$$Z_{V(i-k)} = C^{\mathrm{T}}_{3(i-k)}[V_\xi V_\eta V_\zeta]^{\mathrm{T}}_{(i-k)\mathrm{SINS}} - [V_E V_N V_H]^{\mathrm{T}}_{(i-k)\mathrm{SNS}}; \quad (2)$$

$$Z_{V(i-k)} = H_{(i-k)} x_{(i-k)} + \vartheta_{(i-k)} = H_{(i-k)} \Phi^{-1}_{(i-k)} x_i + \vartheta_{(i-k)}, \quad (3)$$

where C_3 is the direction cosine matrix that characterizes angular position of the reference semi-wander frame $o\xi\eta\xi$ [2] with respect to the geodetic frame *oENH*; $\Phi^{-1}_{i-k} = \prod_{j=k}^{0} \Phi^{-1}_{i-j}$ is the inverse transition matrix for the vector of SINS errors; $H_{(i-k)} = [H^T_{1(i-k)}\ H^T_{2(i-k)} H^T_{3(i-k)}]^T$ is the matrix of coupling between the vector $Z_{V(i-k)}$ of observations and the vector of SINS errors; $H_{j(i-k)}$ is the row vector for factors of coupling between the j-th component $Z_{j(i-k)}$ of the vector $Z_{V(i-k)}$ of observations and the vector of the $x_{(i-k)}$ errors; $j = \overline{1,3}$; $k = var$ is the number of clock periods of the delay (lag) of satellite signals with reference to the instant of formation of observations; $\vartheta_{(i-k)}$ is the vector of random observation errors.

Similarly to this procedure, inertial-and-satellite observations of geodetic coordinates are formed, together with their models. It should be noted that direct and inverse transition matrices for the vector of SINS errors are determined via the numerical solution of the following differential equations:

$$\dot{\Phi}_i = A(t)\Phi(t, t_{i-1}); \qquad \dot{\Phi}^{-1}_i = -\Phi^{-1}(t, t_{i-1})A(t)$$

for $\Phi(t_{i-1}, t_{i-1}) = I$, I is an identity matrix, $A(t)$ is the matrix of partial derivatives that are obtained through the variation of SINS equations.

However, the errors of inertial reckoning of the APC polar coordinate D, which have been obtained under flight experiment conditions [4] were as much as 10 cm on the synthesis interval of 5s. Figure 4 depicts the circular error ΔD of reckoning the APC polar coordinate on the interval of aperture synthesis, which has been obtained taking into account the time mismatch of inertial and satellite measurements, where

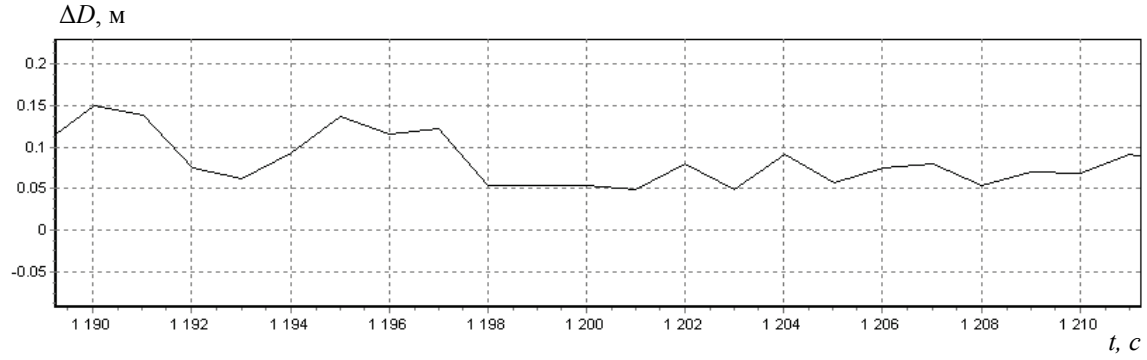

Fig. 4. Error of inertial reckoning of the APC polar coordinate with due regard for the time mismatch ofinertial and satellite measurements

$$\Delta D = \sqrt{\Delta S^2 + \delta^2_{\mathrm{H}}}; \qquad \Delta S = \sqrt{\delta_\varphi{}^2 + \delta_\lambda{}^2}; \qquad \delta_\varphi = (\varphi_{\mathrm{SINS}} - \varphi_{\mathrm{SNS}})\mathrm{R}; \qquad \delta_{\mathrm{H}} = \mathrm{H}_{\mathrm{SINS}} - \mathrm{H}_{\mathrm{SNS}};$$

$\delta_\lambda = (\lambda_{SINS} - \lambda_{SNS}) R \cos\varphi_{SNS}$; $\mathrm{R} = \mathrm{a}\,(1 - 0.5e^2 \sin^2\varphi)$; $\mathrm{a} = 6378245\mathrm{m}$; $e^2 = 0.0066934$;

$\varphi; \lambda; H$ are the APC latitude, APC longitude, and APC elevation above the Earth ellipsoid.

The problem of increasing the resolution of a SAR has necessitated the development of new approaches to the integration of DMNS modules. Taking account of the possibility for retrospective formation of the SAR

aperture, the use of combined procedures for the filtering of observations and for the smoothing of estimates on the synthesis interval is proposed. In this case, improvement of the accuracy of estimation is based on the use of supplementary observations that are obtained in "backward" time.

The purpose of this paper is to study the possibilities for combined processing of observations in "forward" and "backward" time in the interests of improving the accuracy of estimation of SAR path instabilities on the interval of aperture synthesis.

The attainment of the purpose formulated is based on the solution, among the problems mentioned earlier, of the following ones:

- construction of recurrent procedures for optimal smoothing of vectorial state parameters;
- provision of the realizability and computational stability of algorithms for optimal smoothing.

A Technology for the Recurrent Smoothing of Estimates of the Error Vector of a Micronavigation System

The smoothing problem provides for the retrospective refinement of estimates of the state vector (SV), which were obtained at the filtering stage, in the interests of increasing their reliability. However, in a typical RTS (Rauch-Tung-Striebel) algorithm [5], the predicted estimates $\hat{x}_{i/i-1}$ are smoothed, and their reliability is substantially below the corrected estimates $\hat{x}_{i/i}$. Because of this, in [6], a smoothing algorithm for the corrected estimates $\hat{x}_{i/i}$ was developed, which has the following form:

$$\nu_{i/N} = \Phi_{i+1}^{-1}\hat{x}_{i+1/N} - \hat{x}_{i/i}; \tag{4}$$

$$\widetilde{P}_{i+1/N} = P_{i+1/N} + \Gamma_{i+1}Q_i\Gamma_{i+1}^T; \tag{5}$$

$$P_{i/N}^{-1} = \Phi_{i+1}^T\widetilde{P}_{i+1/N}^{-1}\Phi_{i+1} + P_{i/i}^{-1}; \tag{6}$$

$$K_{i/N} = P_{i/N}P_{i/i}^{-1}; \tag{7}$$

$$\hat{x}_{i/N} = \Phi_{i+1}^{-1}\hat{x}_{i+1/N} - K_{i/N}\nu_{i/N}, \tag{8}$$

where $\hat{x}_{i/i}, \hat{x}_{i/N}$ are the estimates x_i of the SV at the *i*-th instant of time, and these estimates are obtained from *i* observations at the stages of filtering and smoothing, respectively; $P_{i/i}; P_{i/N}$ are the covariance matrices of the above estimates; Φ_i is the transition matrix for the SV; *N* is the number of samples taken on the smoothing interval; $Q_i; \Gamma_i$ are the covariance and transition matrices, respectively, for the vector of perturbations in the SP.

The matrix $P_{i/i}^{-1}$ is determined from the solution, in "forward" time, of an informational version of the Riccati equation:

$$P_{i/i}^{-1} = P_{i/i-1}^{-1} + H_i^T R_i^{-1} H_i; \tag{9}$$

$$P_{i/i-1}^{-1} = (\Phi_i P_{i-1/i-1}\Phi_i^T + \Gamma_i Q_{i-1}\Gamma_i^T)^{-1}, \tag{10}$$

where R_i is a covariance matrix for observation errors; H_i is the matrix of coupling of observations and the SV $\hat{x}_{i/i-1}$.

The implementation of algorithm (4) − (10) involves computational difficulties that are caused by the necessity of inverting the covariance matrices $P_{i/i-1}$ and $P_{i/N}$. The above difficulties can be substantially reduced when algorithms for smoothing are realized using the *U-D* technology.

A modification of smoothing algorithm (4) − (10) provides for its representation in the form allowing the replacement of inversions of *n*×*n* covariance matrices by sequences of division operations. Such a replacement relies on the transformation of Eqs. (6), (9), and (10) according to the lemma of matrix inversion [7]. For Eq. (10), it will have the following form:

$$P_{i/i-1}^{-1} = \widetilde{P}_{i/i-1}^{-1} - \widetilde{P}_{i/i-1}^{-1}\Gamma_i(\Gamma_i^T\widetilde{P}_{i/i-1}^{-1}\Gamma_i + Q_{i-1/i-1}^{-1})^{-1}\Gamma_i^T\widetilde{P}_{i/i-1}^{-1} = (\widetilde{P}_{i/i-1} + \sum_j^r \Gamma_j\Gamma_j^T / Q_{jj})^{-1} \tag{11}$$

where $\widetilde{P}_{i/i-1}^{-1} = \Phi_i^{-T}P_{i-1/i-1}^{-1}\Phi_i^{-1}$; Γ_j is the *j*-th column of the *n*×*r* matrix Γ_i; размерности *n*×*r*; Q_{jj} is the *j*-th element of the *r*×*r* diagonal matrix Q_i; $\Phi_i^{-T} = (\Phi_i^{-1})^T$.

Hence, the following procedure for successive realization of Eq. (11) is valid:

$$M_0^{-1} = \Phi_i^{-T} P_{i-1/i-1}^{-1} \Phi_i^{-1} \; ; \tag{12}$$

$$K_j = M_{j\text{-}1}^{-1} \Gamma_j \big/ (\Gamma_j^T M_{j-1}^{-1} \Gamma_j + Q_{jj}^{-1}) ; \tag{13}$$

$$M_j^{-1} = M_{j\text{-}1}^{-1} - K_j \Gamma_j^T M_{j-1}^{-1} ; \tag{14}$$

$$P_{i/i\text{-}1}^{-1} = M_r^{-1} \; ; \; j = \overline{1, r} . \tag{15}$$

A serious drawback of such a representation of Eq. (11) is the presence of the subtraction operation in relation (14), which may lead, because of computational errors, to the loss of positive definiteness of the matrix $P_{i/i-1}^{-1}$. It can be shown that the following quadratic form that eliminates such a drawback is equivalent to relation (14), i.e.,

$$M_j^{-1} = (K_j \Gamma_j^T - I) M_{j-1}^{-1} (K_j \Gamma_j^T - I)^T + K_j Q_{jj}^{-1} K_j^T \; , \tag{16}$$

where I is an $n \times n$ identity matrix.

At present, in the onboard realization of an extended Kalman filter (EKF), its *U-D* modification [8] is a base one and it provides computational stability of the solution of the Riccati equation. The *U-D* technology of filtering was also used in the onboard realization of smoothing algorithms.

Transformations that are similar to (11) − (16) will also hold for Eq. (3) provided the covariance matrix for the errors of filtering is represented as follows:

$$P_{i/i}^{-1} = U_{i/i}^{-T} D_{i/i}^{-1} U_{i/i}^{-1} , \tag{17}$$

where $U_{i/i}$ is an upper triangular matrix with unity diagonal elements; $D_{i/i}$ is a diagonal matrix.

In view of decomposition (17) and a preliminary decomposition of the residuals

$$\tilde{v}_{i/N} = U_{i/i}^{-1} v_{i/N}$$

a *U-D* modification of the combined algorithm for optimal filtering and optimal smoothing can be formed.

Prediction:

$$m_0 = \hat{x}_{i/i-1} = \Phi_i \hat{x}_{i-1/i-1} ; \; j := 1;$$

$$MWGS \left\{ \begin{array}{l} \overline{W}_i = \left[\Phi_i \; U_{i\text{-}1/i\text{-}1} \vdots \Gamma_i \right] \\ \overline{D}_i = diag \; (D_{i\text{-}1/i\text{-}1}, \; Q_{i-1}) \end{array} \right\} \rightarrow \; U_0 ; \; D_0$$

$$j = \overline{1, r} ; \qquad f_j = \Gamma_j U_{j-1}^{-T} ; \; V_j = D_{j-1}^{-1} f_j^T ; \quad K_j = U_{j-1}^{-T} V_j / (f_j V_j + Q_{jj}^{-1}) ;$$

$$MWGSL \left\{ \begin{array}{l} \tilde{W}_j = [K_j f_j \text{-} U_j^{-T} \vdots K_j] \\ \tilde{D}_j = diag \; (D_j^{-1}, \; Q_{jj}^{-1}) \end{array} \right\} \rightarrow \; U_j^{-T} ; \; D_j^{-1}$$

$$U_0^{-T} := U_{i/i\text{-}1}^{-T} = U_r^{-T} ; \; D_0^{-1} := D_{i/i\text{-}1}^{-1} = D_r^{-1} .$$

Updating: $j = \overline{1, l}$; $f_i = H_j \; U_{j\text{-}1} ; \; V_j = D_{j\text{-}1} f_j^{\mathrm{T}} ;$

$$\tilde{\alpha}_j = f_j V_j + R_j \; ; \; K_j = U_{j\text{-}1} V_j / \tilde{\alpha}_j \; ;$$

$$m_j = m_{j\text{-}1} + K_j (z_j - H_j m_{j-1}) ;$$

$$MWGS \left\{ \begin{array}{l} \overline{W}_j = [K_j f_j \text{-} U_{j\text{-}1} \vdots K_j] \\ \overline{D}_j = diag(D_{j\text{-}1}, \; R_j) \end{array} \right\} \rightarrow U_j ; \; D_j$$

$$MWGSL \left\{ \begin{array}{l} \tilde{W}_j = [U_{j-1}^{-T} \vdots H_j^T] \\ \tilde{D}_j = diag(D_{j-1}^{-1}, \; R_j^{-2}) \end{array} \right\} \rightarrow U_j^{-T} ; \; D_j^{-1} \quad .$$

Recording: $\hat{x}_{i/i} = m_l = \tilde{z}_i ; \; U_{i/i} = U_l ; D_{i/i} = D_l ; \; U_{i/i}^{-T} = U_l^{-T} ; \; D_{i/i}^{-1} = D_l^{-1} ; \; j = \overline{1, l} .$ (18)

Interpolation: $m_0 = \hat{\tilde{x}}_{k-1/k} = \Phi_k^{-1}\hat{x}_{k/k}$; $\quad \nu_{k-1} = \tilde{z}_{k-1} - \hat{\tilde{x}}_{k-1/k}$;

$$MWGS\left\{\begin{array}{c}\overline{W}_0 = [\Phi_{i+1}^{-1}U_{i+1/N} \vdots \Phi_{i+1}^{-1}\Gamma_{i+1}] \\ \overline{D}_0 = diag(D_{i+1/N}, Q_i)\end{array}\right\} \rightarrow \begin{array}{c}\tilde{U}_0 \\ \tilde{D}_0\end{array}.$$

Smoothing: $\tilde{\nu}_j = U_j^{-1}\nu_{k-1}$; $\quad f_j = U_j^{-1}\tilde{U}_{j-1}$; $\quad V_j = \tilde{D}_{j-1}f_j^T$;

$$\alpha_{sj} = f_j V_j + D_j \qquad \tilde{K}_j = \tilde{U}_{j-1}V_j / \alpha_{sj};$$

$$MWGS\left\{\begin{array}{c}\overline{W}_j = [(\tilde{K}_j f_j - \tilde{U}_{j-1}) \vdots \tilde{K}_j] \\ \overline{D}_j = diag(\tilde{D}_{j-1}; D_j)\end{array}\right\} \rightarrow \begin{array}{c}\tilde{U}_j \\ \tilde{D}_j\end{array}$$

$$K_j = \tilde{U}_j \tilde{D}_j \tilde{U}_j^T U_j^{-T} D_j^{-1}; \qquad m_j = m_{j-1} + K_j \tilde{\nu}_j; \quad j = \overline{1,n};$$

$$\hat{\tilde{x}}_{k-1/k-1} = m_n;\ U_{i-1/k} = \tilde{U}_n;\ D_{i-1/k} = \tilde{D}_n; \quad k = \overline{i, i-N+1},$$

where U_j^{-1} is the j-th row of the matrix $U_{i/i}^{-1}$; *MWGS* is the procedure for orthogonal transformation [8, 9] of the combination of the $n\times(n+r)$ rectangular matrix $\overline{W}_j$ and the $(n+r)\times(n+r)$ diagonal matrix $\overline{D}_j$ into the combination of the upper triangular matrix $\tilde{U}_j$ with unit diagonal elements and the $n\times n$ diagonal matrix $\tilde{D}_j$; *MWGSL* is a procedure that is similar to the *MWGS* one, which is intended to form the lower triangular matrix U_j^{-T} with unit diagonal elements and the diagonal matrix D_j^{-1}; H_j is the row vector for coupling factors of the observation z_j and the SV m_j.

In smoothing on the moving time interval $T = [t_{i-N+1}, t_i]$, a file both of the estimates $\hat{x}_{i/i}$ and of the appropriate matrices $U_{i/i}, D_{i/i}, U_{i/i}^{-T}$ and $D_{i/i}^{-1}$ is recurrently updated when the next in turn observations z_i become available. For this purpose, the above-mentioned files formed from previous observations are shifted back in time by one step. The updating procedure is so realized that the earliest files are discarded, and the next estimates and matrices corresponding to them are substituted instead of the latest ones.

Analysis of the Results of Flight Development of the Integrated Micronavigation System for a SAR

Flight experiments were conducted using a helicopter. The results of comparative analysis have been obtained on a basis of reckoning motion parameters both from the recorded IMU signals and from the data of SNS and FCNC of the helicopter.

The cyclogram of DMNS system operation included the following stages: coarse initial alignment (t = 0 ÷ 10s); fine realignment (FRA) (t =10 ÷ 900s); navigational mode (t > 900 s).

At the stage of coarse initial alignment, from "a priori" information about the alignment, angular position of the IMU is approximately determined with respect to the axes of the FCNC SINS. Under "FRA+Navigation" conditions, errors of IMU angular position with respect to the navigation moving frame, together with residual drifts of sensors, such as gyros and accelerometers are estimated and compensated for. In the "FRA+Navigation" operating mode, the following problems have also been solved:

- estimation and compensation of DMNS errors from inertial-and-satellite observations, like (2), of position and velocity with a frequency of 1 Hz;
- recording and recurrent updating of vector-matrix data files (18);
- interpolation and smoothing of the estimates of DMNS errors;
- formation of corrections to SAR signals.

The employment of an external special computer has made it possible to implement, in real time, a combined algorithm both for the reckoning of motion parameters of the APC and for the estimation of their errors. The vector of DMNS errors contains 18 parameters, namely: errors in reckoning of components of the vector of relative velocity, errors in reckoning of elements of the quaternions for navigation and attitude, angular drifts of FOGs, biases of accelerometers, and error in the reckoning of altitude with reference to the Earth ellipsoid.

Some of the results of experiments are presented in the following figures: in Fig. 5, a flight path in the horizontal plane is shown, where $\Delta\varphi_R = [\varphi(t) - \varphi(t_0)]R \quad \Delta\lambda_R = [\lambda(t) - \lambda(t_0)]R\cos\varphi$; in Fig. 6, the variation of the component of the vector of path velocity along the oE axis of the moving frame *oENH* of the geodetic coordinate system is depicted; in Figs. 7, 8, the angles of pitch and roll are shown, respectively; in Fig. 9, estimation of the *ox* FOG residual drift is presented; in Fig. 10, estimation of the accelerometer *ox* bias is shown. The figures presented confirm the existence of aircraft path instabilities, the necessity of their determination and compensation for in the process of RADS aperture synthesis.

Figure 11 shows the variation of the position error ΔS over the whole flight path, which was obtained with account for writing off estimates of the vector of DSINS errors.

Figure 12 shows the error of reckoning the "APC-Object" polar coordinate ΔD on the interval of aperture synthesis with due regard both for the lag of SNS signals and for the recurrent smoothing of estimates of the vector of DSINS errors. It can be seen that the processing of inertial-and-satellite observations with due regard for the time mismatch of the signals of the DSINS and SNS, and also for the writing off smoothed estimates of the vector of errors provides uninterrupted (with a frequency that is ≥ 200 Hz) determination of the "APC-Object" polar coordinate at a level of several units of centimeters.

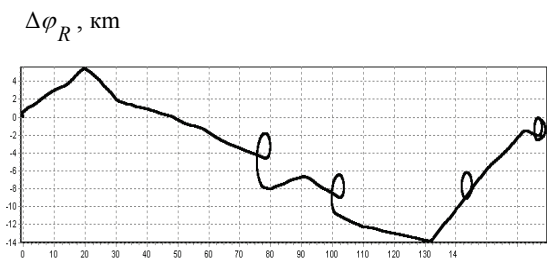

Fig. 5. Flight path in the horizontal plane

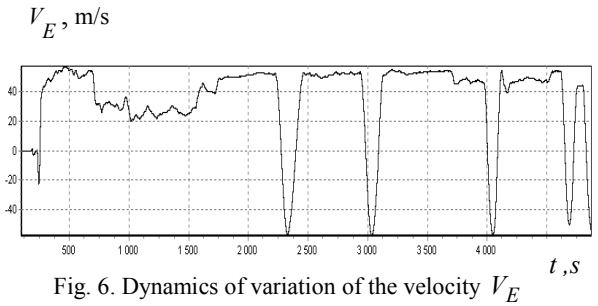

Fig. 6. Dynamics of variation of the velocity V_E

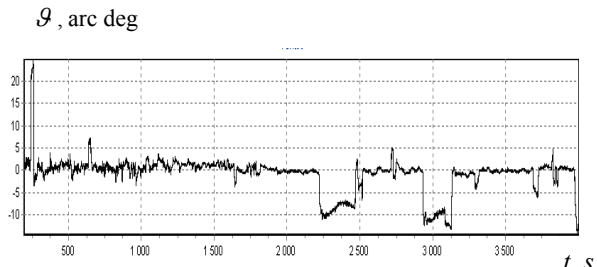

Fig. 7. Angle of pitch

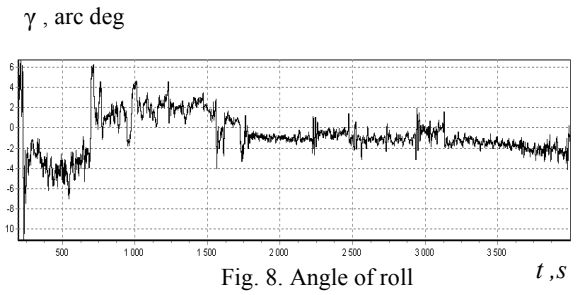

Fig. 8. Angle of roll

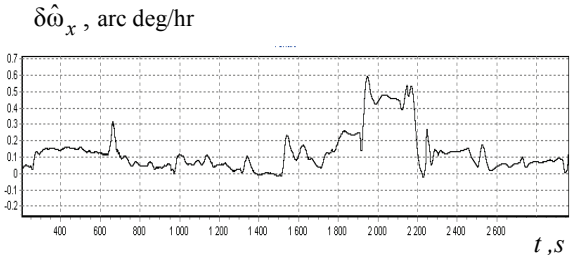

Fig. 9. Estimation of the *ox* FOG residual drift

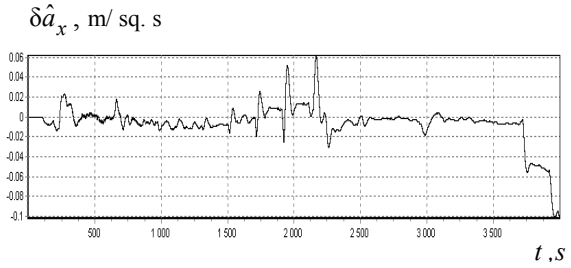

Fig. 10. Estimation of the *ox* accelerometer bias

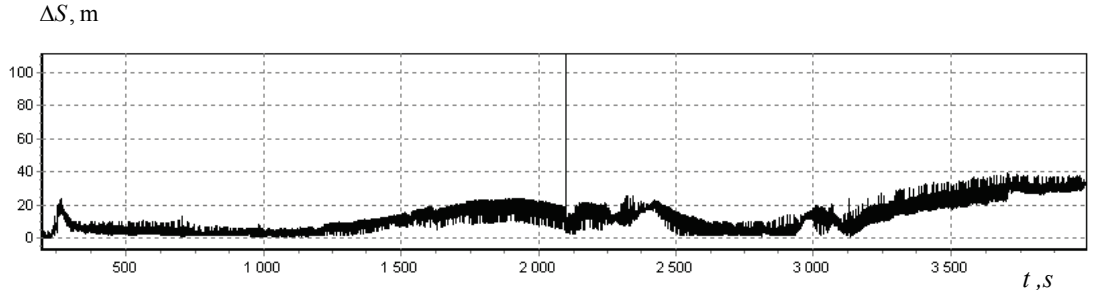

Fig. 11. DSINS circular position error with due regard for the writing off estimates of the vector of errors

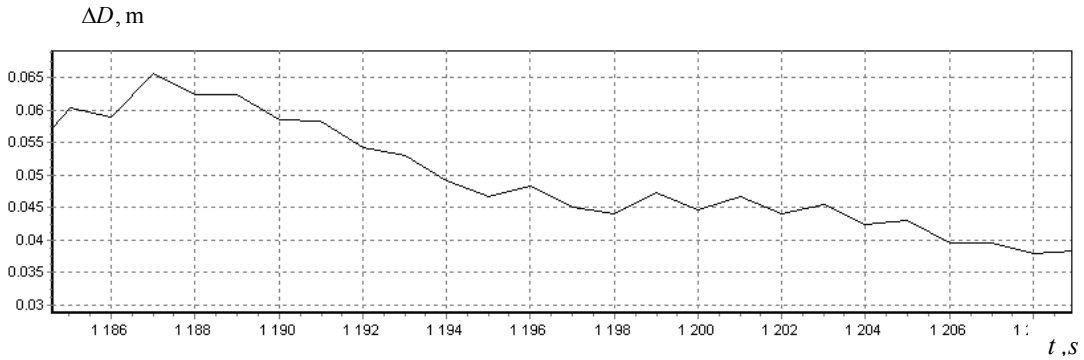

Fig. 12. Error of reckoning the APC polar coordinate with due regard both for the time mismatch of inertial and satellite measurements, and also for the smoothing of estimates of DSINS errors

It can be seen from Fig. 12 that the relative position error on the synthesis interval of 5s was no more than 5mm.

Conclusions

Synthesis of the antenna aperture is one of the promising trends for radar development. The major advantage of this trend is a multiple increase in the RADS angular resolution. In this case, there is the feasibility of detection and radio-vision of small-size objects, of improvement in the accuracy and noise immunity of the RADS. Compensation for aircraft path instabilities in RADS signals can be provided by the use of an inertial satellite micronavigation system with due regard for SAR actual flight operating conditions. For providing the required SAR resolution, it is apparently also expedient to determine a rational relation between the DMNS accuracy characteristics and the range of SAR wavelengths.

References

1. **Aviatsionnye** sistemy radiovideniya (Aircraft Systems for Radio-Vision), Kondratenkov, G.S., Ed., Moscow, Radiotechnika, 2015.
2. **Babich, O.A.,** Obrabotka informatsii v navigatsionnykh kompleksakh (Data Processing for Navigation Complexes), Moscow, Mashinostroenie, 1991.
3. **Bilik, V.V., Kovregin, V.N., Chernodarov, A.V., and Patrikeev, A.P.,** A Spatially Distributed Micronavigation System for a Synthetic-Aperture Radar, 18th St. Petersburg International Conference on Integrated Navigation Systems, St. Petersburg, CSRI Elektropribor, 2011, pp. 207-215.
4. **Chernodarov, A.V., Patrikeev, A.P., Kovregin, V.N., and Kovregina, G.M.,** Synchronization of Inertial and Satellite Measurements in the Micronavigation System for a Synthetic-Aperture Radar 22th St. Petersburg International Conference on Integrated Navigation Systems, St. Petersburg, CSRI Elektropribor, 2015, pp. 127-130.
5. **Rauch, H.E., Tung, F., and Striebel, C.T.,** Maximum Likelihood Estimates of Linear Dynamic Systems, AIAA Journal, 1965, vol. 3, no. 8, 1445–1450.
6. **Chernodarov, A.V., Enyutin, V.V., and Patrikeev A.P.,** Diagnosis of Integrated Navigation Systems on a Basis of the Joint *U* - *D* Procedures of Filtering and Smoothing, Giroskopiya i Navigatsiya, 2000, no.3, pp. 34-48.
7. **Sage, A.P., and White, C.C.,** Optimum Systems Control, New Jersey, Prentice – Hall, 1977.
8. **Bierman, G.J.,** Factorization Methods for Discrete Sequential Estimation, New York., Academic Press, 1977.
9. **Kolodezny, L.P., and Chernodarov, A.V.,** Nadezhnost' i tekhnicheskaya diagnostika (Reliability and Engineering Diagnostics), Moscow, Zhukovsky and Gagarin Air Force Academy, 2010.